Appl. Phys. B 73, 745–750 (2001)
DOI: 10.1007/s003400100727

Applied Physics B
Lasers and Optics

V.A. KAPITANOV[1,✉]
YU.N. PONOMAREV[1]
K. SONG[2]
H.K. CHA[2]
J. LEE[2]

Resonance photoacoustic spectroscopy and gas analysis of gaseous flow at reduced pressure

[1] Institute of Atmospheric Optics SB RAS, 1 Akademicheskii Ave., 634 055 Tomsk, Russia
[2] Laboratory for Quantum Optics, Korea Atomic Energy Research Institute, 150 Duckjin-dong, Yusong, Taejon 305-600, Korea

Received: 19 April 2001/Revised version: 18 September 2001
Published online: 7 November 2001 •

ABSTRACT The results of theoretical and experimental studies of sensitivity of a resonant photoacoustic Helmholtz resonator detector for gas flowing through a photoacoustic cell under reduced pressure are presented. The measurements of the sensitivity and ultimate sensitivity of the differential photoacoustic cell were performed with a near-IR room-temperature diode laser using the well-known H_2O absorption line (12 496.1056 cm^{-1}) as a reference. The measured value of the sensitivity (6–17 Pa W m^{-1}) is in satisfactory agreement with the calculated one, which equals 6–35 Pa W m^{-1}. The obtained value of the ultimate sensitivity ($(3–5) \times 10^{-7}$ W m^{-1} $Hz^{-1/2}$) provides measurements of the concentration of molecules at the ppb–ppm level.

PACS 07.07, 07.60

1 Introduction

Spectroscopic methods of gas analysis are of considerable current use in solving problems of monitoring the gaseous content and pollutants of the atmosphere. Thanks to extremely high sensitivity, wide dynamical range, and comparatively simple mechanical realization, laser photoacoustic (PA) spectroscopy has considerable promise in constructing spectroanalytical instruments for monitoring atmospheric pollution. The ultimate sensitivity of the photoacoustic apparatus fully depends on the design of the PA cell and parameters of the adopted laser source. As sources, high-power molecular gas lasers find the widest application at the present time.

When constructing PA cells, such phenomena of the acoustic resonance in a cell volume are commonly used such as, for example, excitation of longitudinal modes at single-path [1–3] or intracavity [4] illumination of the PA cell, radial modes [5, 6], and azimuth modes in the open (free of windows) PA cell [7]. The resonant PA cells give us the following possibilities [8]:

1. Improvement of the signal/noise (S/N) ratio and in some cases exclusion of windows at all;
2. Realization of a continuous gas blowing through the PA detector cell [5];
3. Minimization of the adsorption of gaseous molecules under study on the PA cell walls;
4. Determination of the relaxation and thermodynamic characteristics of the gas under study.

The design of the resonant PA cells is rather sophisticated, which allows, in particular, suppressing the external acoustic noise caused by the gas flow through the cell. It was proposed [9–11] to use a simple PA cell made as a differential Helmholtz resonator (DHR) in the flow mode. The DHR allows a doubling of the signal amplitude and a significant, at least by an order of magnitude, decrease of external noise.

In the range of pressures close to atmospheric, at which the gas blowing through the cell of the resonant PA detector is measured, the spectral line broadening by pressure places essential limits on the spectral selectivity of the method. This is of particular importance in those spectral ranges where significant absorption by molecules of the main atmospheric gases, such as water vapor and CO_2, takes place. At the reduced pressure P in the PA cell, the line width decreases proportionally to $\sim P^{-1}$, and the possibility appears of distinguishing the absorption lines of the pollutants from the absorption lines of the main atmospheric components. Within the pressure range $\sim 10^4$ Pa, the density decrease of the gas under measurement is compensated by narrowing of the spectral line; therefore, the decrease of the absorption coefficient in the line center becomes insignificant, i.e. of the order of 30%–50%.

The magnitude of the ultimate sensitivity of the PA spectrometer–gas analyzer, which is given by

$$(k_v)_{min} = (\sigma_v \times c_{min}) = \frac{\sqrt{U_n^2}}{R_c \times R_m \times W_0} \quad (1)$$

at standard pressure, is mainly determined by the characteristics of the acoustic resonator. Here σ_v is the absorption cross section, c_{min} is the minimally detectable concentration of pollution, $\sqrt{U_n^2}$ is a r.m.s. value of noise intensity at the preamplifier input, R_c is the resonant-cell sensitivity, R_m is the microphone sensitivity, and W_0 is the power of the laser source.

This paper presents the results of theoretical and experimental studies of sensitivity of the resonant PA DHR detector as applied to detection of trace gases in the atmosphere, as

✉ Fax: +7-38/2225-8026, E-mail: kvan@asd.iao.ru

well as to the spectroscopy of flowing gas in PA cells of flow and flow-less types at reduced pressure.

2 PA DHR cell

The PA cell with high sensitivity acting as the Helmholtz resonator (HR) in monitoring air pollution was designed by the present authors (Fig. 1). This type of resonator consists of two volumes connected by a capillary. As compared to other resonators, the Helmholtz resonator's advantage is in using cells of small volume with low resonance frequency and the possibility of improving the S/N ratio by using differential schemes [9–11].

The PA HR detector consists of two identical cells equipped with Knowles electric microphones EK 3027 ($R_\mathrm{m} = 0.02\,\mathrm{V/Pa}$) connected by two identical capillaries (Fig. 2a). Such a design gives a possibility to carry out flow measurements if the difference between the microphones is measured. To predict the acoustic properties and sensitivity of the PA HR detector, a theoretical model based on an acoustic analogy to an electric line circuit was used. We have shown in our work that the electric circuit approach is a very efficient method to study the acoustic resonance and describe the HR and DHR characteristics with the experimental accuracy [9–11].

3 Theory

An acoustic wave in the PA HR detector is generated by absorption of radiation of a chopper laser beam. Under the assumption that the acoustic wavelength exceeds the overall dimensions of the cell, the corresponding electric line circuit is represented by discrete circuit elements [12]. The pressure amplitude P and the volume velocity are replaced in this circuit by the voltage amplitude U_mic and the electric current I_0. Since the acoustic wave excitation is due to the heat of the absorbing power in the cell $W \times k_\mathrm{v} \times L$, the current source I_0 is expressed as [11]

$$I_0 = \left\{(\gamma - 1)/(2.22 \times \varrho \times U^2)\right\} \times W_0 \times k_\mathrm{v} \times L \qquad (2)$$

where W_0 is the laser power, k_v is the absorption coefficient of the gas, L is the cell length, ϱ is the gas density, and $\gamma = C_p/C_v$ is the ratio of specific heats at constant pressure and volume. The pressure amplitudes U_m at the position of the microphones are determined as

$$U_\mathrm{m} = Z \times I_0 \qquad (3)$$

where Z is the acoustic impedance of the acoustic volume (cell).

The potentiality of any photoacoustic detector is completely determined by such an important parameter as the sensitivity $\Lambda = \sqrt{U_\mathrm{n}^2}/R\,(\mathrm{W\,m^{-1}\,Hz^{-1/2}})$, where $\sqrt{U_\mathrm{n}^2}\,(\mathrm{V\,Hz^{-1/2}})$ is the r.m.s. value of noise, e.g. intrinsic noise of the microphone (Johnson, Brownian, and thermal noises), circuit noise, and external acoustic noise.

Since the cell absorption is low ($k_\mathrm{v} \times L \ll 1$) and the exciting radiation power does not achieve the absorption saturation level, the sensitivity R is a magnitude of the electric signal produced by the microphone for a unit of the power absorbed by molecules per unit length. The ultimate sensitivity Λ is the noise equivalent power of the photoacoustic detector, defined as the minimum magnitude of the absorbed power, which can be detected at $\mathrm{S/N} = 1$ at the given frequency and given frequency band.

Sensitive electric microphones are commonly used in measuring pressure oscillations, and the sensitivity of the PA detector can be represented as the product of the microphone sensitivity R_m and the cell sensitivity $R_\mathrm{c} = U_\mathrm{m}/W_0 \times k_\mathrm{v}$, $R = R_\mathrm{c} \times R_\mathrm{m}$. The cell sensitivity is determined as

$$R_\mathrm{c} = U_\mathrm{m}/W_0 \times k_\mathrm{v} = Z \times \left\{(\gamma \times l)/(2.22 \times \varrho \times U^2)\right\} \times L\,. \qquad (4)$$

If the acoustic wavelength is comparable with the spatial dimensions of the resonator, a longitudinal standing sound wave occurs in the cavity. In this case, the modeling by the discrete acoustic impedance fails, and the Helmholtz resonator should be treated in terms of the extended Helmholtz resonator (EHR) theory [13]. This approach considers sound-wave propagation in the cells and capillaries. The correct impedance of a tube can be calculated by dividing the tube into subcells of infinitesimal length. Connection of the infinitesimal subcells in series yields the characteristic impedance Z_ω and the propagation constant γ_ω of an electric transmission line, which describes a sound wave propagating through the tube.

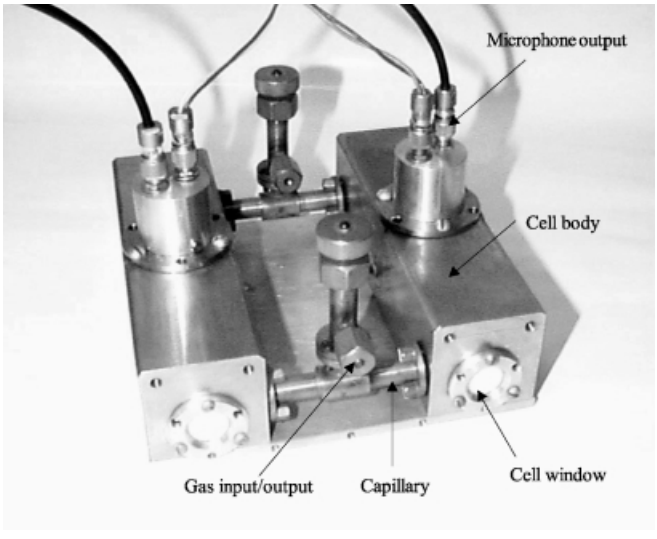

FIGURE 1 Photoacoustic detector with a differential Helmholtz resonant (DHR) cell

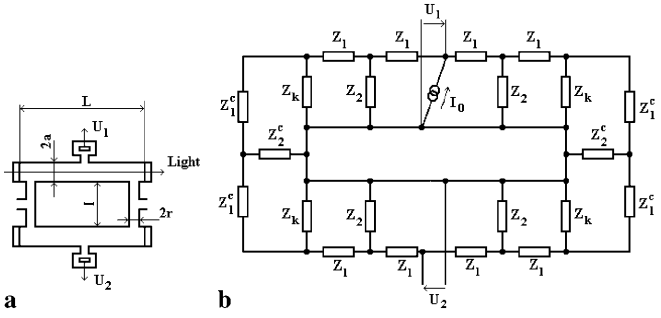

FIGURE 2 Schematic representation of the DHR photoacoustic cell (**a**) and its analogous electric line circuit (**b**)

Retransformation of an electric transmission line into a simple circuit consisting of discrete acoustic elements of the cell Z_i and of the capillary Z_i^{c} yields the electric line circuit of the EHR (Fig. 2b). Expressions for calculation of the characteristic impedances Z_ω (cell) and Z_ω^{c} (capillary), propagation constants γ_ω and $\gamma_\omega^{\mathrm{c}}$, and discrete acoustic impedances Z_i and Z_i^{c} are given in [14]:

$$Z_\omega = \frac{\varrho U}{\pi a^2}\left[\frac{1+\frac{d_{\mathrm{v}}}{a}}{1+(\gamma-1)\frac{d_{\mathrm{t}}}{a}}\right]^{1/2} \times\left[1-\frac{\mathrm{i}}{2}\left(\frac{\gamma-1}{\frac{a}{d_{\mathrm{v}}}+1}-\frac{\gamma-1}{\frac{a}{d_{\mathrm{t}}}+(\gamma-1)}\right)\right];$$

$$\gamma_\omega = \frac{\mathrm{i}\omega}{U}\left[\left(1+\frac{d_{\mathrm{v}}}{a}\right)\left(1+(\gamma-1)\frac{d_{\mathrm{t}}}{a}\right)\right]^{1/2} \times\left[1-\frac{\mathrm{i}}{2}\left(\frac{\gamma-1}{\frac{a}{d_{\mathrm{t}}}+(\gamma-1)}+\frac{1}{\frac{a}{d_{\mathrm{v}}}}\right)\right]; \quad (5)$$

$$Z_1 = Z_\omega \tanh\left(\frac{\gamma_\omega L}{4}\right); \quad Z_2 = \frac{Z_\omega}{\sinh\left(\frac{\gamma_\omega L}{2}\right)};$$

$$Z_\omega^{\mathrm{c}} = \frac{\varrho U^2}{\pi R^2}\left[\frac{1+\frac{d_{\mathrm{v}}}{r}}{1+(\gamma-1)\frac{d_{\mathrm{t}}}{r}}\right]^{1/2} \times\left[1-\frac{\mathrm{i}}{2}\left(\frac{\gamma-1}{\frac{r}{d_{\mathrm{v}}}+1}-\frac{\gamma-1}{\frac{r}{d_{\mathrm{t}}}+(\gamma-1)}\right)\right];$$

$$\gamma_\omega^{\mathrm{c}} = \frac{\mathrm{i}\omega}{U}\left[\left(1+\frac{d_{\mathrm{v}}}{r}\right)\left(1+(\gamma-1)\frac{d_{\mathrm{t}}}{r}\right)\right]^{1/2} \times\left[1-\frac{\mathrm{i}}{2}\left(\frac{\gamma-1}{\frac{r}{d_{\mathrm{t}}}+(\gamma-1)}+\frac{1}{\frac{r}{d_{\mathrm{v}}}}\right)\right]; \quad (6)$$

$$Z_1^{\mathrm{c}} = Z_\omega^{\mathrm{c}} \tanh\left(\frac{\gamma_\omega l}{2}\right); \quad Z_2^{\mathrm{c}} = \frac{Z_\omega^{\mathrm{c}}}{\sinh(\gamma_\omega L)};$$

$Z_k \to \infty$ close cell

$Z_k \to 0$ open cell (7)

Here $\omega = 2\pi f$ is the circular modulation frequency of the laser beam, U is the sound velocity, and U_{m1} and U_{m2} are signal amplitudes of the microphones.

The thicknesses d_{v} and d_{t} of the viscous and thermal boundary layers of the cell and capillary walls are described by the expressions

$$d_{\mathrm{v}} = \sqrt{\frac{2\mu}{\varrho\times\omega}}; \quad (8)$$

$$d_{\mathrm{t}} = \sqrt{\frac{2K}{\varrho\times\omega\times c_p}}; \quad (9)$$

where μ is the viscosity and K is the heat conductivity of the buffer gas.

Calculated according to (4)–(9), the sensitivities vs. modulation frequency f of nonresonant and longitudinal resonant cells are shown in Fig. 3. The acoustic impedances of nonresonant Z_0 and resonant Z_l cells are defined as follows:

$$Z_0 = \frac{1}{\mathrm{i}C2\pi f}; \; C = \frac{V}{\varrho U^2}; \quad (10)$$

$$Z_l = \frac{1}{2}\left[Z_1 + \frac{Z_2(Z_1+Z_k)}{Z_1+Z_2+Z_k}\right], \quad (11)$$

where $V = \pi a^2 l$ is the cell volume and Z_1, Z_2, and Z_k are calculated by means of (5) and (7).

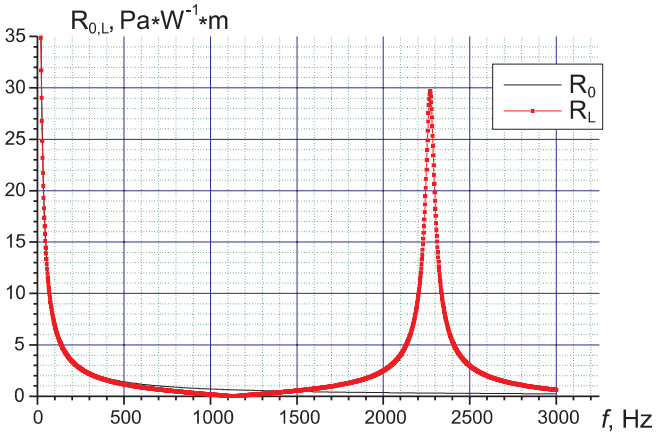

FIGURE 3 Calculated cell sensitivity of nonresonant R_0 and longitudinal resonant R_{L} cells vs. modulation frequency f. Cell pressure is one atmosphere

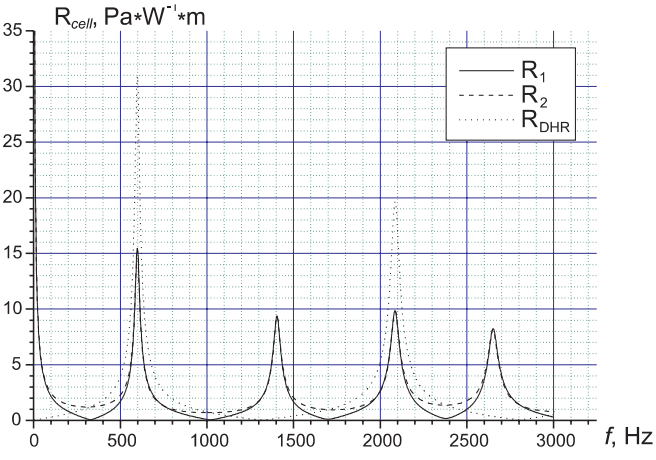

FIGURE 4 Calculated cell sensitivity of DHR cell R_{DHR} vs. modulation frequency f. Cell pressure is one atmosphere

Figure 4 presents the calculated sensitivities vs. modulation frequency f for the DHR cell (Figs. 1 and 2) when signals $U_{\mathrm{m}i}$ from one of the microphones or a difference of signals $U_{\mathrm{m1}} - U_{\mathrm{m2}}$ are measured. The specifications for the DHR cell and the buffer gas N_2 at atmospheric pressure are given by:

Cell length L, (m)	0.150
Cell radius a, (m)	0.0036
Capillary length l, (m)	0.0984
Capillary radius r, (m)	0.0030
Mass density ϱ, (kg m^{-3})	1.1662
Velocity of sound U, (m s^{-1})	346
Thermal conductivity k, (W m^{-1} K^{-1})	0.02598
Specific heat capacity C_v, (J kg^{-1} K^{-1})	718
$\gamma = C_p/C_v$	1.4
Viscosity μ, (kg m^{-1} s^{-1})	1.79×10^{-5}

At atmospheric pressure the sensitivity R_{DHR} of the PA cell slightly exceeds the sensitivity R_{L} of the PA cell with longitudinal resonance.

As has been shown [9–11], due to recording the difference between the signals from microphones located in different DHR cells and subtraction of in-phase external noise, the r.m.s. noise value for the DHR cell is lower than that for nonresonant and longitudinal resonant PA cells and, correspondingly, the ultimate sensitivity Λ is 1–2 orders of magnitude lower. This is of particular importance in the regime of continuous gas flow through the PA cell.

Within the pressure region 1–100.3 kPa, the gas elasticity significantly changes. Since such thermodynamic characteristics of the medium as viscosity, heat conductivity, heat capacity, adiabatic exponent, and sound velocity only slightly depend on the pressure, the magnitude of the sensitivity $R_{\mathrm{DHR}}(f)$ and the value of the resonance frequency f_0 are determined by the pressure and temperature dependence of the medium density

$$\varrho = \frac{m}{R_{\mathrm{g}} \times T} P \,, \tag{12}$$

where m is the molar weight, R_{g} is the gas constant, P is the buffer gas pressure, and T is the gas temperature.

Figure 5a presents the frequency dependence of the sensitivity R_{DHR} calculated for reduced pressures. Decrease of gas pressure in the DHR cell from 701.3 kPa to 2.66 kPa results in a significant (six-fold) decrease of the sensitivity $R_{\mathrm{DHR}}(f_0)$ and 10% change of the resonance frequency. At the same time, up to 2.66 kPa, inclusive, the peculiarities of the Helmholtz resonance (Fig. 5b) and phase opposition of pressure oscillations within different cells remain invariable; the DHR cell sensitivity therewith is two times higher than that of the HR cell and five times higher than the sensitivity of some isolated cell.

4 Experiment

Measurements of the sensitivity R_{DHR} and the ultimate sensitivity Λ_{DHR} of the PA DHR detector at atmospheric and reduced pressures were conducted using the PA spectrometer with a near-IR diode laser (Fig. 6). The laser radiation (0.8 μm) of the room-temperature diode laser (EOSI 2001-ECU), modulated by a mechanical chopper (HMS light beam chopper model 220), passes one of the cells of the DHR detector. The laser-radiation power is recorded with an IR detector (Newport 818-BB-20). The range of continuous linear tuning of the laser-radiation wavelength is $\sim 1.5\ \mathrm{cm}^{-1}$ in the region 12 430–12 580 cm^{-1}, and the initial wavelength is measured with a wavelength meter (Burleigh WA-20-VIS). The microphone signals U_{m1}, U_{m2}, and $U_{\mathrm{m1}} - U_{\mathrm{m2}}$, as well as the signal of the IR detector W, are amplified and detected with lock-in amplifiers (EG&G 5210, $\tau = 1$ s) and then recorded with an analog-to-digital converter (Stanford Research Systems 245).

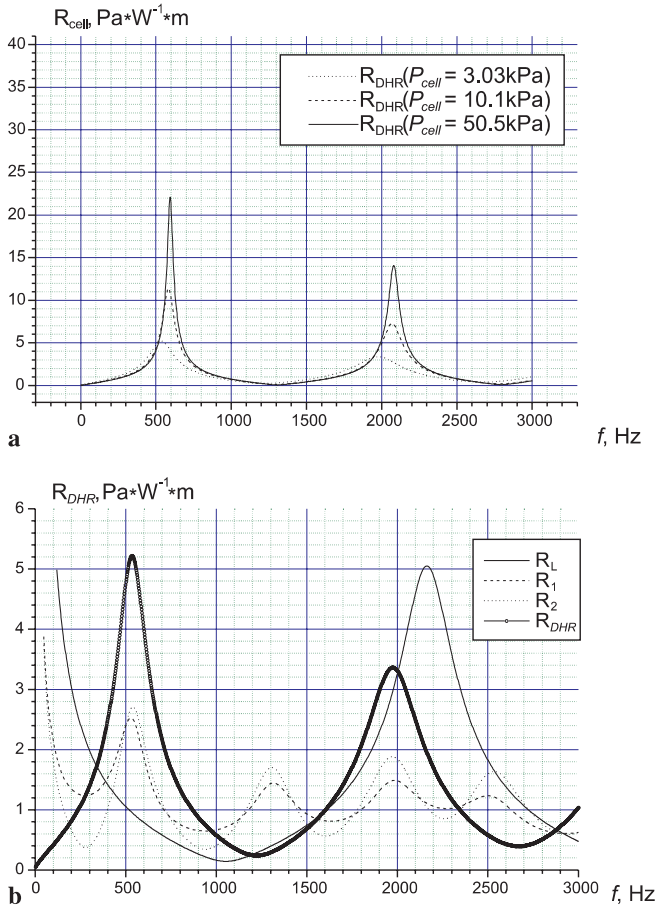

FIGURE 5 Calculated cell sensitivity of DHR cell R_{DHR} vs. modulation frequency f at different pressures in the cell (**a**) and sensitivities of longitudinal resonant R_{L}, Helmholtz resonant R_i, and differential Helmholtz resonant R_{DHR} cells at reduced pressure ($P_{\mathrm{cell}} = 2.66$ kPa) (**b**)

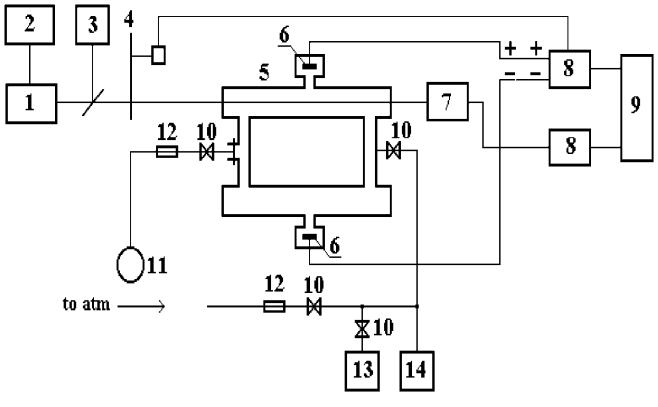

FIGURE 6 Experimental setup diagram of the diode-laser spectrometer: 1, 2 – diode laser and its control unit; 3 – wavelength meter; 4 – mechanical chopper; 5 – DHR PA detector; 6 – microphones; 7 – power meter; 8 – lock-in amplifiers; 9 – recorder; 10 – vacuum valves; 11 – vacuum pump; 12 – capillaries; 13 – vessel with water; 14 – vacuum gauge

The vacuum system used allows measurements of the PA detector characteristics under flow and flow-less operation modes. The flow operation mode (continuous blowing of gas through the measurement cell) at atmospheric and reduced pressures was made with the use of two volume-controllable capillaries (1×10^{-6}–1.33×10^{-4} m^3 kPa/s). The pressure at the cell input was measured with a vacuum manometer (MKS Babatron type 127).

5 Results and discussion

To determine the sensitivity and the ultimate sensitivity of the PA DHR detector, the absorption coefficient of the well-known H_2O absorption line ($\nu_0 = 12\,496.1056\,\mathrm{cm}^{-1}$, $\gamma_L = 0.106\,\mathrm{cm}^{-1}\,\mathrm{atm}^{-1}$, $S = 0.58 \times 10^{-6}\,\mathrm{cm}^{-2}\,\mathrm{atm}^{-1}$, $\gamma_D = 0.018\,\mathrm{cm}^{-1}$, $T = 293$ K) was measured. Here ν_0 is the line center, γ_L is the Lorenz broadening coefficient, S is the line intensity, and γ_D is the Doppler HWHM. The examples of the measurements at atmospheric and reduced pressures are presented in Fig. 7a, b. The H_2O absorption line shape was obtained at the mean power of the diode laser of $\sim 5.4 \times 10^{-3}$ W. The experimental data were processed with the use of standard package 'Origin 5.0'. Each absorption line was approximated by the Voigt contour, and the values of the r.m.s. intensity of noise and the amplitude difference between the microphones' signals were found from this fitting. Figure 8a, b presents the experimental and the calculated (by (4)) dependences of the cell sensitivity and the noise levels on pressure.

Estimation of the DHR cell sensitivity R_{DHR} (Fig. 8a, experimental) was made in supposition that the microphone sensitivity R_m is independent of pressure. Nevertheless, as shown in [15], it may well depend on pressure and increase as the pressure falls [9–11]. On the one hand, this leads to overestimation of the cell sensitivity at reduced pressure; on the other, taking into account the decrease of noise level (Fig. 8b), this results in a very weak pressure dependence of the ultimate sensitivity of the PA DHR detector (Fig. 8c).

Suppression of the external acoustic noise caused by continuous gas flow through the PA cell of the DHR detector at atmospheric pressure and a flow rate of 0.5 L/min has been demonstrated in [10]. Figure 9a,b demonstrate some examples of water-vapor absorption line ($\nu_0 = 12\,496.11\,\mathrm{cm}^{-1}$) registration in the regime of continuous air flow at the input pressure $P \cong 2.666$ kPa and the air rate in the capillary of 1.33×10^{-4} m^3 kPa/s for the cases of measuring a signal from one of the microphones (Fig. 9a) and measuring the difference between signals from both microphones (Fig. 9b). The second peak close to $12\,496.4\,\mathrm{cm}^{-1}$ (Fig. 9a) represents a striking example of interference acoustic effects due to blowing gas when the signal from one of the microphones is

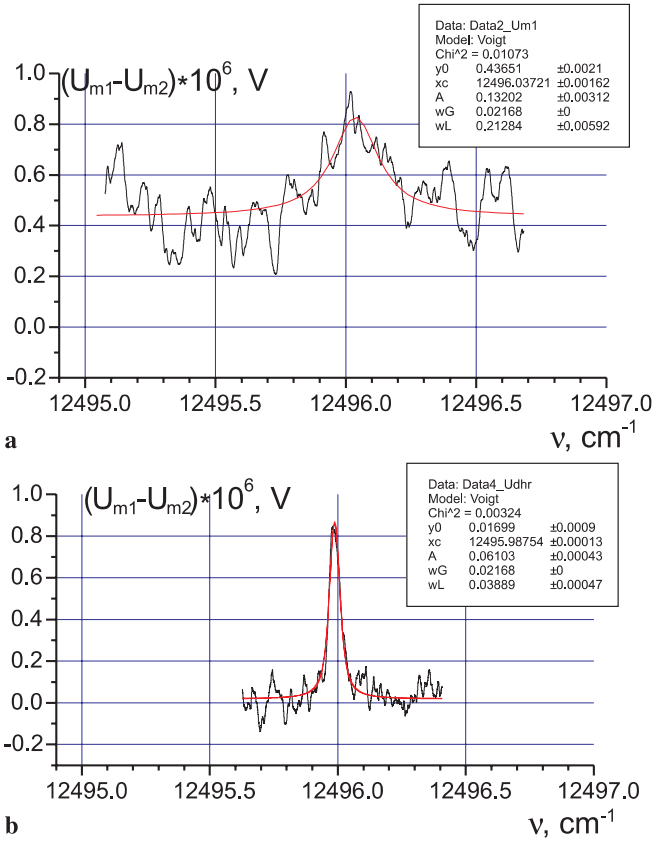

FIGURE 7 Examples of photoacoustic spectrum of water vapor (no flow): **a** at the atmospheric pressure of the buffer gas ($P_{H_2O} = 1.33$ kPa), **b** at the reduced pressure of the buffer gas ($P_{buffer} = 1.33$ kPa, $P_{H_2O} = 1.8$ kPa, $P_{cell} = 3.13$ kPa)

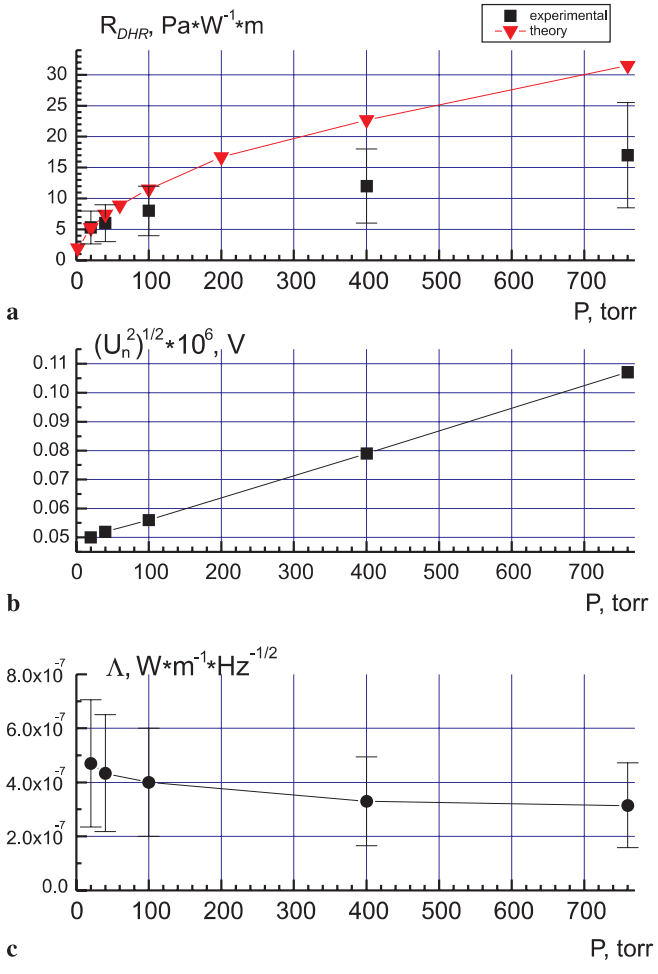

FIGURE 8 Sensitivity R_{DHR} (**a**), r.m.s. noise level $\sqrt{U_n^2}$ (**b**), and ultimate sensitivity Λ (**c**) vs. cell pressure

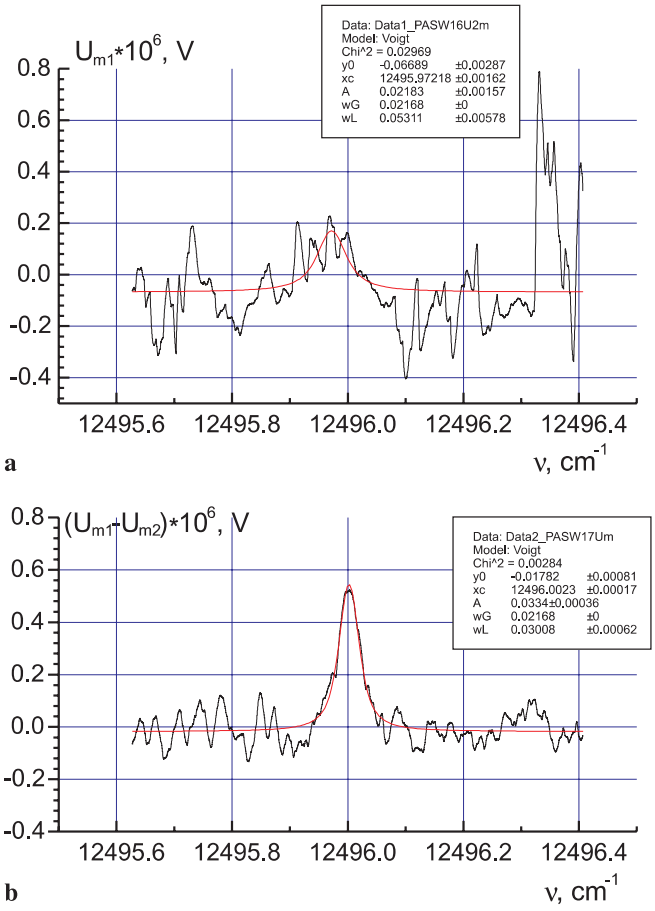

FIGURE 9 Examples of photoacoustic spectrum of water vapor at the gas flow ($P_{\text{cell}} = 2.13$ kPa, $P_{H_2O} = 0.9$ kPa): **a** only one microphone signal is measured, **b** the difference between microphones is measured

measured. The S/N ratio for the DHR detector exceeds by almost an order of magnitude the ratio for the HR detector, and the intensity of r.m.s. noise in both cases (flow and flow-less operation modes) remains constant.

The PA DHR cell is constructed specially to achieve a fast time response and a low threshold of sensitivity, as well as to suppress the external acoustic noise due to the blowing gas. The gas flow passes through two cells under the same conditions and generates a cophased acoustic noise in them, which is suppressed by a differential amplifier. Although only one cell of the PA detector is illuminated by a laser ray, the acoustic waves, opposite in phase at the Helmholtz resonance frequency, are generated in both cells of the detector. Signals, entering from the microphones located in the center of each cell, are subtracted by the differential amplifier, doubling therewith the valid signal and, correspondingly, the sensitivity R_c of the PA cell [10, 11].

Due to the efficient suppression of the outer acoustic signals and the increase of the cell sensitivity, the obtained value of the threshold sensitivity of the PA DHR detector $(K_v)_{\min} \times W_0$ in the gas flow under atmospheric pressure is $3 \times 10^{-7}\,\mathrm{W\,m^{-1}}$. The value is comparable with $(K_v)_{\min} \times W = 1.0 \times 10^{-7}\,\mathrm{W\,m^{-1}}$ for the differential cell given in [16] and lower than the threshold sensitivity of the resonance cell $(K_v)_{\min} \times W = 1.8 \times 10^{-6}\,\mathrm{W\,m^{-1}}$ [4]. Generally speaking, there is a possibility for a two-fold decrease of the PA DHR ultimate sensitivity by means of the optical scheme with a mirror chopper [10]. At lowered pressures in the PA cell, the gas-analysis selectivity significantly increases because of spectral line narrowing. Thus, the results of investigations of the PA DHR cell threshold sensitivity at low pressures are of great interest. The threshold sensitivity of the cell only slightly depends on the pressure and is equal to $5 \times 10^{-7}\,\mathrm{W\,m^{-1}}$ in the gas flow at the input pressure of $P_{\text{cell}} = 2.13$ kPa.

The presented results count in favor of high potentialities of the PA DHR (along with other resonance cells) in trace-gas analysis.

REFERENCES

1 M. Feher, Y. Jiang, J.P. Maier, A. Miklós: Appl. Opt. **33**, 1655 (1994)
2 R.A. Rooth, A.J.L. Verhage, L.W. Wouters: Appl. Opt. **29**, 3643 (1990)
3 J. Henningsen, T. Møgelberg, M. Hammerich: J. Phys. IV 4, C7.499 (1994)
4 F.J.M. Harren, F.G.C. Bijnen, J. Reuss, L.A.C.J. Voesenek, C.W.P.M. Blom: Appl. Phys. B: Photophys. Laser Chem. **50**, 137 (1990)
5 P.L. Meyer, M.W. Sigrist: Rev. Sci. Instrum. **61**, 1779 (1990)
6 A. Thony, M.W. Sigrist: Infrared Phys. Technol. **36**, 585 (1995)
7 G.Z. Angeli, Z. Bozoki, A. Miklos, A. Lorincz, A. Thony, M.W. Sigrist: Rev. Sci. Instrum. **62**, 810 (1991)
8 V.P. Zharov, V.S. Letokhov: *Laser Optoacoustic Spectroscopy* (Springer, Berlin 1986)
9 A.B. Antipov, V.A. Kapitanov, Yu.N. Ponomarev, V.H. Sapozhnikova: *Optoacoustic Method in Laser Molecular Spectroscopy* (Nauka, Novosibirsk 1984) p. 128
10 V. Zeninari, V.A. Kapitanov, Yu.N. Ponomarev, D. Courtois: Infrared Phys. Technol. **40**, 1 (1999)
11 Yu.N. Ponomarev, B.G. Ageev, M.W. Sigrist, V.A. Kapitanov, D. Courtois, O.Yu. Nikiforova: *Laser Optoacoustic Spectroscopy of Intermolecular Interaction in Gases* (SSI RASKO, Tomsk 2000) p. 199
12 O. Nordhaus, J. Pelzl: Appl. Phys. **25**, 221 (1981)
13 J. Pelzl, K. Klein, O. Nordhaus: Appl. Opt. **21**, 94 (1982)
14 R. Kastle, M.W. Sigrist: Appl. Phys. B **63**, 389 (1996)
15 I.G. Calasso, M.W. Sigrist: Rev. Sci. Instrum. **70**, 4569 (1999)
16 A. Miklos, P. Hess: Rev. Sci. Instrum. **72**, 1937 (2001)